OPEN

Prostate Cancer and Prostatic Diseases (2016) 19, 349–357

www.nature.com/pcan

ORIGINAL ARTICLE

Reversible lysine-specific demethylase 1 antagonist HCI-2509 inhibits growth and decreases c-MYC in castration- and docetaxel-resistant prostate cancer cells

S Gupta[1], A Weston[1], J Bearrs[1], T Thode[1], A Neiss[1], R Soldi[2] and S Sharma[1]

BACKGROUND: Lysine-specific demethylase 1 (LSD1 or KDM1A) overexpression correlates with poor survival and castration resistance in prostate cancer. LSD1 is a coregulator of ligand-independent androgen receptor signaling promoting *c-MYC* expression. We examined the antitumor efficacy of LSD1 inhibition with HCI-2509 in advanced stages of prostate cancer.
METHODS: Cell survival, colony formation, histone methylation, c-MYC level, *c-MYC* expression, cell cycle changes and *in vivo* efficacy were studied in castration-resistant prostate cancer cells upon treatment with HCI-2509. *In vitro* combination studies, using HCI-2509 and docetaxel, were performed to assess the synergy. Cell survival, colony formation, histone methylation and c-myc levels were studied in docetaxel-resistant prostate cancer cells treated with HCI-2509.
RESULTS: HCI-2509 is cytotoxic and inhibits colony formation in castration-resistant prostate cancer cells. HCI-2509 treatment causes a dose-dependent increase in H3K9me2 (histone H3lysine 9) levels, a decrease in c-MYC protein, inhibition of *c-MYC* expression and accumulation in the G0/G1 phase of the cell cycle in these cells. PC3 xenografts in mice have a significant reduction in tumor burden upon treatment with HCI-2509 with no associated myelotoxicity or weight loss. More synergy is noted at sub-IC_{50} (half-maximal inhibitory concentration) doses of docetaxel and HCI-2509 in PC3 cells than in DU145 cells. HCI-2509 has growth-inhibitory efficacy and decreases the c-myc level in docetaxel-resistant prostate cancer cells.
CONCLUSIONS: LSD1 inhibition with HCI-2509 decreases the c-MYC level in poorly differentiated prostate cancer cell lines and has a therapeutic potential in castration- and docetaxel-resistant prostate cancer.

Prostate Cancer and Prostatic Diseases (2016) **19,** 349–357; doi:10.1038/pcan.2016.21; published online 28 June 2016

INTRODUCTION

The efficacy of androgen deprivation therapy in high-risk metastatic prostate cancer is short lived, and tumors evolve during treatment with androgen deprivation therapy to become castration-resistant.[1] Treatment with abiraterone, enzalutamide, radium-223, sipuleucel-T and taxane-based chemotherapy provide additional survival benefit;[2] however, castration-resistant prostate cancer (CRPC) eventually progresses and remains the second-leading cause of cancer death in men.[3]

Epigenetic processes have a significant role in embryonic pluripotency, cellular differentiation, cancer progression and epithelial–mesenchymal transition. Lysine-specific demethylase 1 (LSD1), the first histone demethylase enzyme identified, can either function as a corepressor or a coactivator of transcriptional regulation depending on its association with differing binding partners. In association with CoREST[4] and NuRD,[5] it demethylates mono- and dimethyl histone H3lysine 4 (H3K4me1 and H3K4me2), resulting in transcriptional repression. When LSD1 partners with nuclear androgen or estrogen hormone receptors, it switches its substrate specificity to mono- and dimethyl histone H3lysine 9 (H3K9me1/me2), resulting in transcriptional activation.[6] As an androgen receptor (AR) coregulator, LSD1 has a significant role in both hormone-dependent[6] and -independent[7,8] prostate cancer.

LSD1 also mediates epithelial–mesenchymal transition and resistance to chemotherapy in mouse hepatocyte cell cultures. Demethylation of H3K9me2 allows derepression of large heterochromatin domains and enables transcription of genes that confer a survival advantage in a challenging cellular environment.[9]

LSD1 is overexpressed in poorly differentiated prostate cancer and predicts poor survival.[10] As prostate cancer progresses through treatment modalities of androgen deprivation and chemotherapy, it acquires a progressively more stem cell-like character.[11] AR signaling continues to have a significant role as a driver of CRPC by various mechanisms such as AR gene amplification,[12,13] constitutionally active AR splice variants[14,15] local androgen production and hijacking of AR signaling by other oncogenic pathways and ligands.[16,17] LSD1 colocalizes with the AR in prostate cancer cells and has a critical role in AR signaling, with *c-MYC* oncogene as a crucial ligand-independent AR target gene.[18] c-Myc signaling has a significant role in mediating castration resistance,[19] epithelial–mesenchymal transition and docetaxel resistance[20] in prostate cancer cells.

Targeting epigenetic mechanisms to treat advanced stages of prostate cancer is an attractive strategy. DNA demethylation,[21] bromodomain inhibition[18] and HDAC inhibition[22] have been studied in this context.

In this study, we investigate the growth-inhibitory effects of HCI-2509 in PC3 and DU145 cell lines. These cell lines have been derived from poorly differentiated metastatic prostate cancer,

[1]GU Medical Oncology, Division of Medical Oncology, Huntsman Cancer Institute, University of Utah, Salt Lake City, UT, USA and [2]Beta Cat Pharmaceuticals, Houston, TX, USA. Correspondence: Dr S Gupta, GU Medical Oncology, Division of Medical Oncology, Huntsman Cancer Institute, University of Utah, 2000 Circle of Hope, Ste 2163, Salt Lake City, UT 84112, USA.
E-mail: sumati.gupta@hci.utah.edu
Received 16 February 2016; revised 16 May 2016; accepted 17 May 2016; published online 28 June 2016

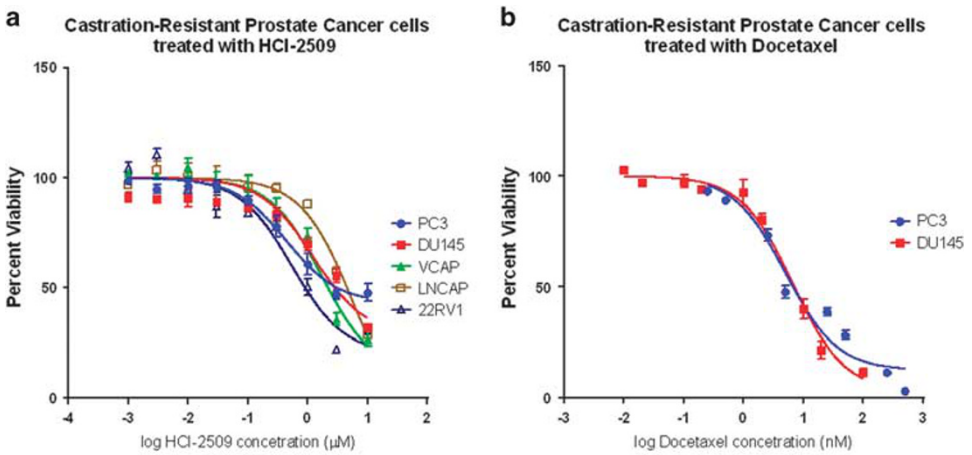

	IC50 HCI-2509 (μM)
PC3	0.438
DU145	1.226
VCAP	2.183
LNCAP	4.435
22RV1	1.092

	IC50 Docetaxel (nM)
PC3	5.094
DU145	6.784

Figure 1. Effects of HCI-2509 and docetaxel on cell survival in prostate cancer cell lines. The logarithmic drug concentration was plotted versus the percent cell survival and half-maximal inhibitory concentrations (IC_{50}s) were calculated by nonlinear regression analysis using GraphPad Prism (GraphPad Software, San Diego, CA, USA). Dose–response curves showing the percent cell viability at the end of 72 h treatment in (**a**) VCAP, LNCAP, 22RV1, PC3 and DU145 cells with HCI-2509, and (**b**) PC3 and DU145 cells with docetaxel.

have low AR gene expression and low levels of AR protein.[23] AR signaling continues to have a significant central role in the CRPC regulatory network in both of these cell lines.[24]

HCI-2509 is a potent, reversible and selective LSD1 inhibitor with demonstrated preclinical efficacy in Ewing's sarcoma,[25] acute myeloid leukemia[26] and endometrial cancer.[27] HCI-2509 is the lead compound for preclinical studies targeting LSD1 developed from a novel series of LSD1 inhibiting N′-(1-phenylethylidine)-benzo hydrazide compounds.[28] Our initial screening studies with several different prostate cancer cell lines revealed cytotoxicity with this class of LSD1 inhibitors. PC3 and DU145 cells represent two distinct groups with regard to clusters of cellular phenotypes in CRPC. These clusters are derived from CRPC gene expression data sets and are based on differences in their active CRPC regulatory pathways.[24] For the purpose of our studies, we have chosen these poorly differentiated CRPC cell lines and a docetaxel-resistant prostate cancer cell line as representative of areas of unfulfilled clinical need in this disease.

MATERIALS AND METHODS

Cell culture and cell viabilities

Human prostate cancer cell lines LNCAP, VCAP, 22RV1, PC3 and DU145 were obtained from American Type Culture Collection (ATCC, Manassas, VA, USA) and cultured in Roswell Park Memorial Institute (RPMI) medium supplemented with 10% fetal bovine serum, 100 U ml^{-1} penicillin and 100 μg ml^{-1} streptomycin at 37 °C in a humidified atmosphere containing 5% CO_2. Cells were seeded in triplicate in 96-well plates at a density of 5000 cells per well, allowed to adhere overnight and then treated with either vehicle (1% dimethyl sulfoxide (DMSO) in RPMI) or increasing concentrations of HCI-2509 (Center for Investigational Therapeutics, Huntsman Cancer Institute, Salt Lake City, UT, USA). After incubation for 72 h, cell viability was assessed using CellTiter-Glo (Promega, Madison, WI, USA).

Further experiments were performed with the CRPC cell lines PC3 and DU145. Cell viabilities of these cell lines were tested using docetaxel (Selleck Pharmaceuticals, Houston, TX, USA).

Colony formation assays

Colony formation assays were performed in duplicate in 6-well plates for each cell line treated with either vehicle (1% DMSO) or serially increasing concentrations of HCI-2509 ranging from 1 nM to 1000 nM at the time of setting up the assay. Using stock solutions of 1.6% agarose (SeaPlaque GTG agarose from Lonza, Allendale, NJ, USA) and 2× RPMI (RPMI powder; Life Technologies, Grand Island, NY, USA), an underlayer constituted by 0.8% agarose in RPMI was prepared. An overlayer of 5000 treated cells per well suspended in 0.4% agarose in RPMI was prepared. After incubation for 3 weeks, colonies were photographed and counted.

Western blot

Cells were seeded (1×10^6) in 10 cm dishes. Once 50% confluent, these were treated with vehicle (1% DMSO) or HCI-2509 at increasing concentrations of 1, 3 and 10 μM for 24 to 48 h. Treated cells were lysed, their protein extracted and immunoblotted with the following antibodies: β-actin mouse mAb: LI-COR (Lincoln, NE, USA) 926-42212; dimethyl histone H3 (K9) rabbit mAb: Cell Signaling 9753S; *c-MYC* rabbit mAb: Cell Signaling (Boston, MA, USA) 9402S.

RNA isolation and quantitative PCR

Cells were seeded (1×10^6) in 10 cm dishes. Once 50% confluent, these were treated with 1% DMSO or 1 μM of HCI-2509 for 4 and 24 h. Total RNA was extracted from the cells using an RNeasy Plus Kit (Qiagen, Valencia, CA, USA). cDNA was generated using High Capacity cDNA Reverse Transcription Kit (Applied Biosystems, Boston, MA, USA). This was then amplified, detected and quantified using SYBR green fluorescence (SYBR Green PCR Master Mix; Applied Biosystems) using the ViiA 7 Real-Time PCR System (Boston, MA, USA). The following primers were used: 18S (Thermo Fisher, Boston, MA, USA; Hs03928990_g1) and c-MYC (Thermo Fisher; Hs00153408_m1).

Cell cycle

Cells in active growth phase were treated with vehicle (1% DMSO), HCI-2509 at varying concentrations (1, 3 and 10 μM), docetaxel at 100 nM or a combination of HCI-2509 (10 μM) plus docetaxel (100 nM) for 24 h. Cells were harvested, fixed in ethanol, stained with propidium iodide and then

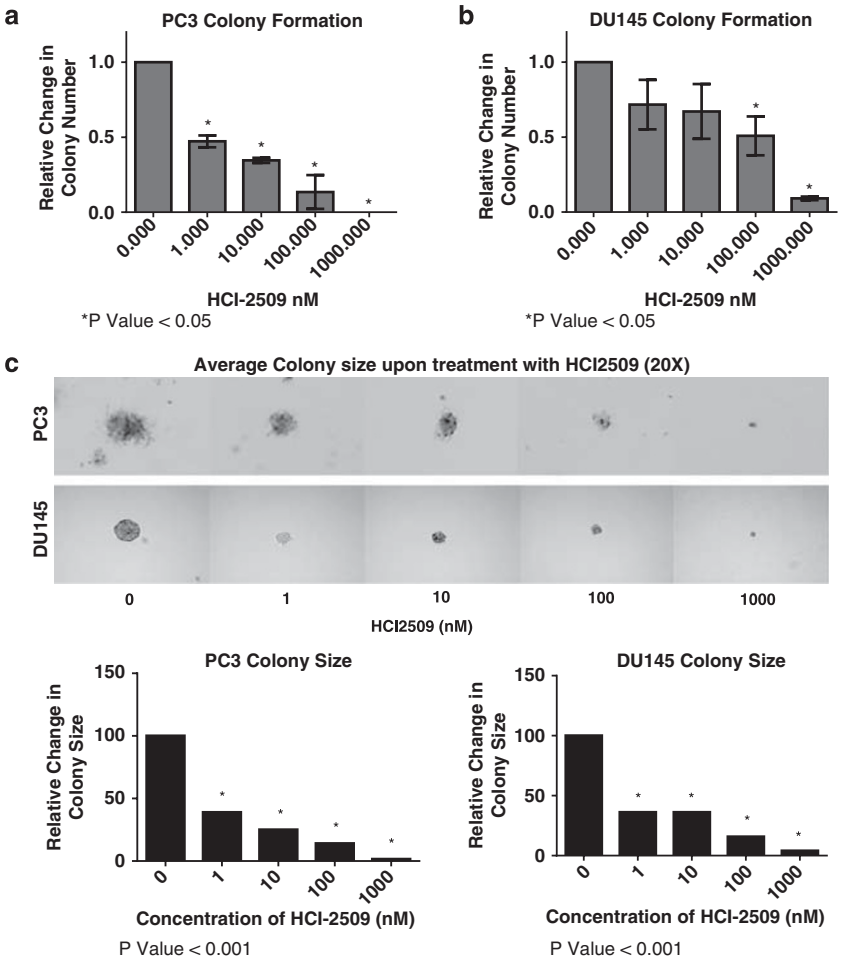

Figure 2. Effect of HCI-2509 on colony formation using soft agar assays in castration-resistant prostate cancer cells. A bar graph was plotted to represent the fractional inhibition of colony formation upon treatment with HCI-2509 compared with vehicle using GraphPad Prism in (**a**) PC3 and (**b**) DU145 cells Assays were performed in duplicate and error bars indicate the standard deviation. Photographs demonstrate average colony size at × 20 magnification with different doses of HCI-2509 in each cell line (**c**), with quantification of colony size plotted as a bar graph using GraphPad Prism. Student's unpaired *t*-tests, using GraphPad Prism software, were used to calculate two-tailed *P*-values for each experiment to determine statistical significance between untreated and treated samples. The statistically significant *P*-values are labeled in each figure with an asterisk.

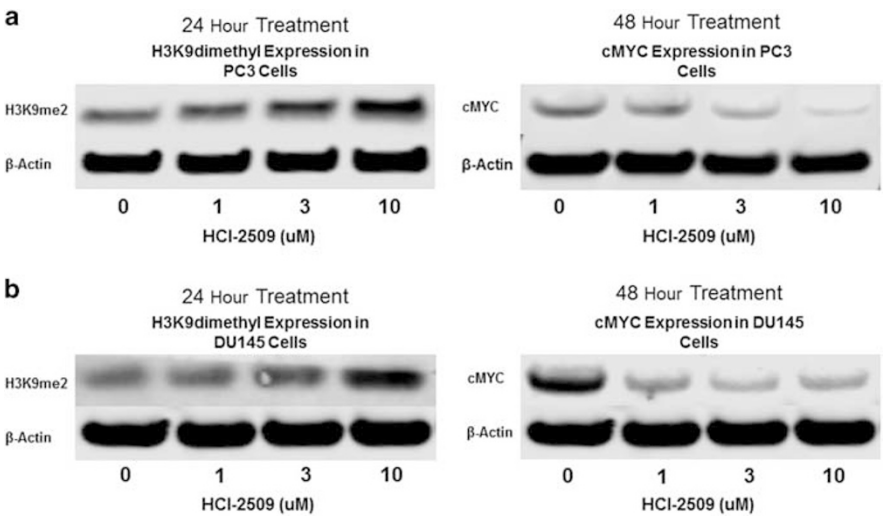

Figure 3. Western blot analysis of H3K9me2 and c-MYC levels upon treatment with increasing concentrations of HCI-2509 as compared with vehicle in (**a**) PC3 and (**b**) DU145 cells. The bands of c-MYC, β-actin and H3K9me2 proteins on the immunoblot were cropped using PowerPoint (Windows) to show correlating change in intensities with different levels of treatment with HCI-2509. (Replicated two more times, representative blot shown).

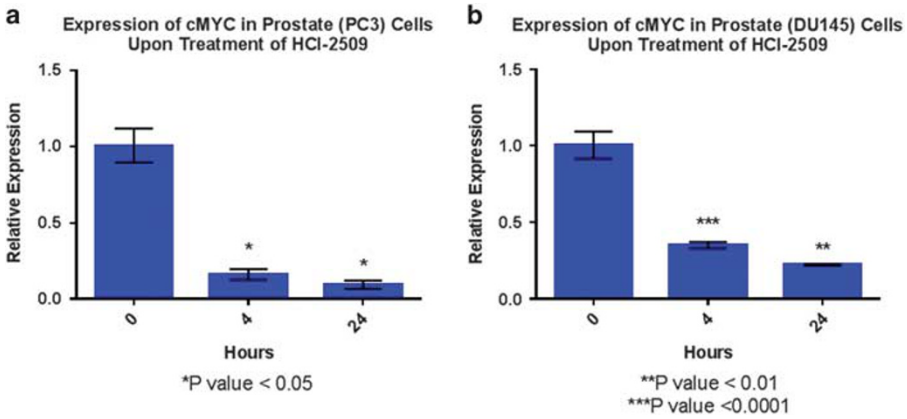

Figure 4. Quantitative reverse transcription-PCR (RT-PCR) analysis of *c-MYC* oncogene in (**a**) PC3 and (**b**) DU145 cells after treatment with HCI-2509 for 4 and 24 h. Each replicate was normalized to the reference gene (S18) and induction was calculated relative to the vehicle control. The relative expression of *c-MYC* mRNA in various conditions was plotted in the form of bar graphs and relative inhibition on treatment with HCI-2509 was tested for significance using the unpaired *t*-test (GraphPad Prism). Assays were performed in quadruplicate and error bars indicate the standard deviation.

analyzed using a BD FACSCanto Analyzer with Software Diva vs6.1.3 (BD Biosciences, San Jose CA, USA).

Xenograft studies

All *in vivo* studies were approved and conducted as per the regulations of the Institutional Animal Care and Use Committee at the University of Utah. Sample size calculation accounted for an attrition rate of 10%. The power calculation was based on a two-tailed test of significance with a type I error of 0.05 and a 0.9 probability of detecting a true difference. This yielded a sample size of 10 animals per arm.

Five million PC3 cells were suspended in 50% media (RPMI) and 50% Matrigel (BD Biosciences), and then implanted in the right hind flank of female nude mice. Animals bearing tumors of adequate size (100 mm^3) were randomized based on size into three cohorts of 10 animals each and dosed with either vehicle intraperitoneally (Monday, Wednesday and Friday), 40 mg kg^{-1} HCI-2509 intraperitoneally (Monday, Wednesday and Friday) or 40 mg kg^{-1} HCI-2509 orally (*per os*) (daily, Monday through Friday) for 3 weeks (last dose administered on Day 19). Body weight and tumor volume were measured twice weekly. Blood cell counts (hematocrit, platelet and white blood cell) were measured on days 1 and 24 using a HemaTrue Hematology Analyzer (Heska, Loveland, CO, USA).

Heat maps

PC3 and DU145 cells were seeded in triplicate in 96-well plates at a density of 5000 cells per well and allowed to adhere overnight. These were then treated with vehicle (1% DMSO), increasing doses of HCI-2509 and docetaxel alone and in a 7×7 combination at seven different dose levels of each drug clustered around the previously calculated half-maximal inhibitory concentration (IC_{50}s). Cell viability was assessed after 72 h of treatment.

Studies on docetaxel-resistant cells

Docetaxel-resistant PC3D12 (PC3D12) cells[29] were obtained, cultured and maintained with 12 nM docetaxel in RPMI growth medium. Cell viabilities, colony formation assays and immunoblotting for c-myc and H3K9me2 upon treatment with HCI-2509 were performed by methods described above.

RESULTS

LSD1 inhibition with HCI-2509 is cytotoxic to prostate cancer cells

A dose-dependent decrease in cell viability is observed after 72 h of treatment with HCI-2509 in all prostate cancer cell lines with IC_{50}s in the high nanomolar to low micromolar range, as shown in Figure 1a.

IC_{50}s for PC3 and DU145 cells using docetaxel are close to 5 nM (Figure 1b).

HCI-2509 is a potent inhibitor of colony formation in CRPC cells

Anchorage-independent growth is inhibited with diminished colony numbers (Figures 2a and b) and size (Figure 2c) in these cells. It is noteworthy that the effect of initial treatment persists for 3 weeks. Anchorage-independent growth is significantly more sensitive to LSD1 inhibition with close to 50% reduction in colony formation at 10 nM concentration. There is complete ablation of colony formation at 1 μM dose of HCI-2509.

LSD1 inhibition affects the concentration of transcriptional regulators

Western blot analysis shows that treatment of PC3 and DU145 cells with HCI-2509 results in a dose-dependent increase in H3K9me2 and decrease in c-MYC protein. (Figures 3a and b).

HCI-2509 inhibits *c-MYC* gene expression in CRPC cells

LSD1 inhibition with HCI-2509 (1 μM) results in inhibition of *c-MYC* gene transcription in PC3 and DU145 cells at 4 and 24 h treatment time-points (Figures 4a and b).

LSD1 inhibition by HCI-2509 affects the cell cycle in CRPC cells

Docetaxel causes a G2M arrest in PC3 and DU145 cells. LSD1 inhibition results in the accumulation of cells in the G0/G1 phase of the cell cycle. Treatment with HCI-2509 and docetaxel simultaneously leads to a bimodal peak in G0/G1 and G2/M for both CRPC cell lines (Figures 5a and b).

PC3 xenografts show *in vivo* efficacy of HCI-2509

Treatment with HCI-2509 both intraperitoneally and *per os* causes a significant reduction in tumor burden in PC3 xenografts (Figure 6a) with progressive weight gain in all three arms (Figure 6b). There is no significant change in the platelet count, white blood cell count or hematocrit (Figures 6c–e) in the treatment arms compared with the control arm.

Combination treatment with docetaxel and HCI-2509 can be synergistic

Treatment with docetaxel and HCI-2509 in combination in CRPC cell lines is synergistic, additive or competitive depending on the

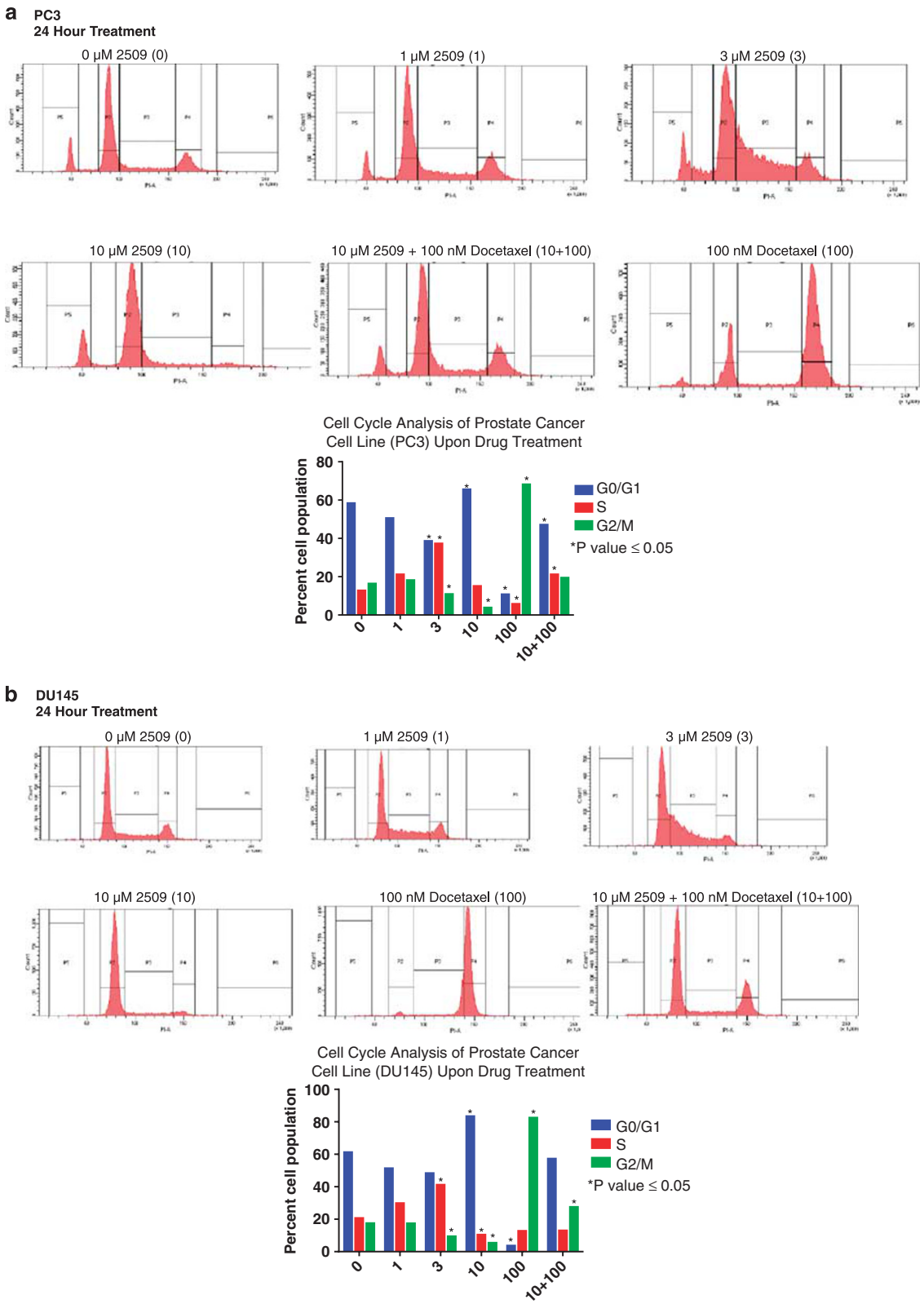

Figure 5. Cell cycle study of percent cell populations in various phases after treatment with vehicle, HCI-2509 in increasing concentrations and docetaxel alone and in combination with HCI-2509 using (**a**) PC3 and (**b**) DU145 cells. Student's unpaired *t*-tests, using GraphPad Prism software, were used to calculate two-tailed *P*-values for each experiment to determine statistical significance between untreated and treated samples. The statistically significant *P*-values are labeled in each figure with an asterisk. (Replicated two more times, representative graph shown).

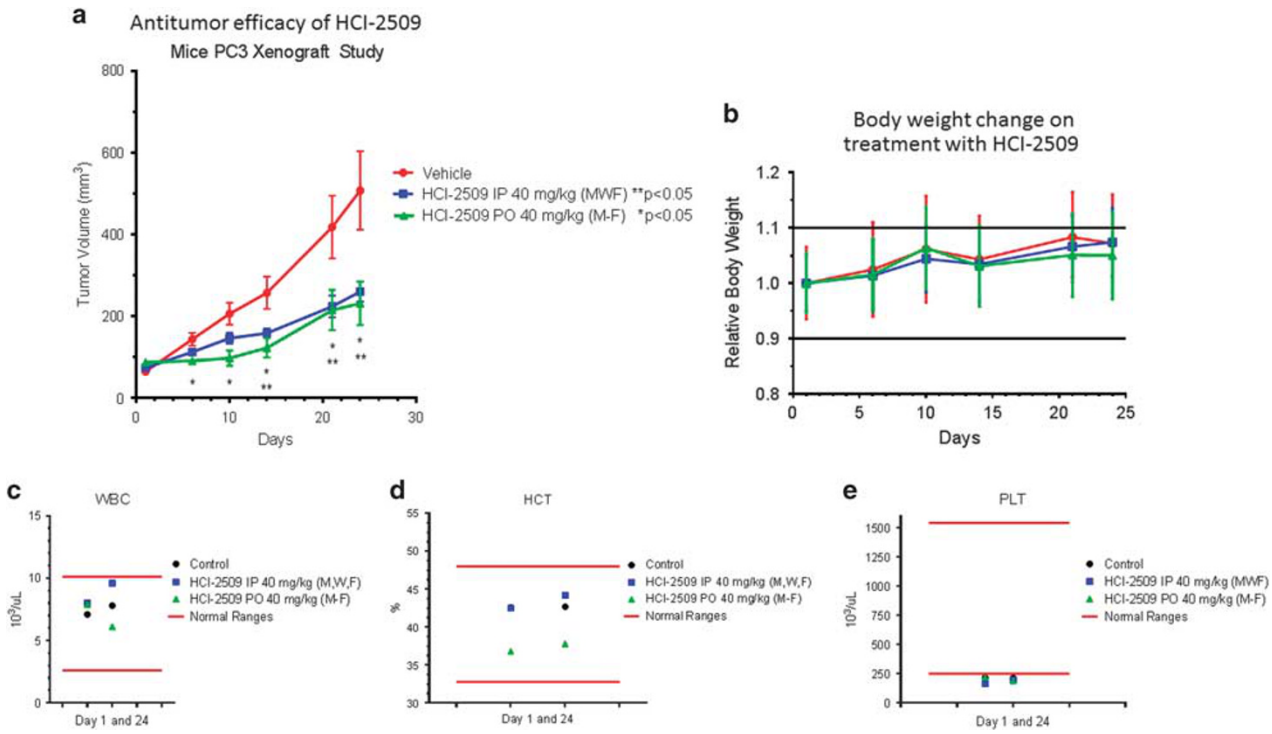

Figure 6. PC3 xenograft study shows efficacy and tolerability of HCI-2509 *in vivo*. (**a**) Tumor volume (TV) plotted versus time in different treatment arms—vehicle, intraperitoneal HCI-2509 and *per os* HCI-2509. The mean TV with error bars to show the standard error of mean (s.e.m.) has been used for the three groups. (**b**) Relative body weight (BW) of mice in the three treatment arms plotted versus time while on study. Relative mean BW with error bars representing s.e.m. in each group are used. Change in (**c**) white blood cell count, (**d**) hematocrit and (**e**) platelet count in the three treatment arms. Data are represented by creating graphs using the GraphPad Prism software. Statistical analysis of the change in mean tumor volume in each arm with time and treatment was performed using two-way analysis of variance (ANOVA) test. The changes in tumor volume with both forms of treatment as compared with control were found to be significant.

concentrations used and the cell line studied. The combination is synergistic at sub-IC_{50} concentrations, with more points of synergy observed in PC3 cells than in DU145 cells. Isobolograms showing the combination points and drug ratios displaying synergy, additivity and competition are presented in Figures 7a–d.

HCI-2509 has similar inhibitory effects in docetaxel-resistant prostate cancer cells

IC_{50} for PC3D12 using docetaxel is >50 nM and the IC_{50} using HCI-2509 is similar to that for CRPC cells with IC_{50}s in the high nanomolar to low micomolar range. Treatment with HCI-2509 potently inhibits colony formation and diminishes colony size in PC3D12 cells. HCI-2509 treatment in these cells results in a dose-dependent increase in H3K9me2 levels and a decrease in c-myc protein concentration.

DISCUSSION

Our studies demonstrate the efficacy of reversible and specific LSD1 inhibition with HCI-2509 in growth inhibition and c-MYC decrease in poorly differentiated castration- and docetaxel-resistant prostate cancer cell lines with low AR expression.

Nonspecific amine oxidase inhibitors inhibit LSD1 but have off-target side effects.[30] Pargyline, an irreversible monoamine oxidase inhibitor, used as an LSD1 inhibitor, does not have any antitumor efficacy in prostate cancer xenograft studies.[31] Cryptotanshinone, another LSD1 inhibitor, downregulates AR signaling. However, its action appears to be dependent on the interaction between androgen ligand, AR and LSD1 and it fails to suppress growth in the absence of DHT in LNCAP (a hormone-sensitive prostate cancer cell line) and castration-resistant PC3 cells.[32] Reversible specific LSD1 inhibition with namoline, a γ-pyrone, is effective in the androgen-sensitive prostate cancer cell line LNCAP and has *in vivo* antitumor efficacy, and also causes weight loss in treated mice.[33] Our studies demonstrate cytotoxicity of HCI-2509 in PC3 and DU145 cell lines with IC_{50}s in the high nanomolar to low micromolar range (Figure 1a).

LSD1 inhibitors have been shown to inhibit pluripotent cancer cells of germ cell tumor origin without affecting normal somatic cells.[34] The remarkable efficacy of HCI-2509 in inhibiting colony formation in our studies (Figures 2a–c) suggests that LSD1 maintains stem cell function in advanced stages of prostate cancer. This finding is reminiscent of the vital role of LSD1 in the maintenance of pluripotency in human embryonic stem cells.[35]

c-MYC is an important androgen ligand-independent AR target gene that contributes to AR-dependent prostate cancer cell survival in CRPC.[18] We demonstrate a dose-dependent decrease in c-MYC protein levels (Figure 3a), with HCI-2509 treatment, correlating with a corresponding increase in H3K9me2 levels (Figure 3b) in castration-resistant cell lines. Quantitative reverse transcription-PCR was performed to evaluate whether the drop in c-MYC protein is due to degradation or a direct effect on gene expression. *c-MYC* gene expression is significantly reduced at 4 and 24 h after treatment with HCI-2509 (1 μM) (Figure 4).

Downregulation of c-MYC has been shown to rescue tumor cells from chemotherapy and radiation in some studies[36] and increase sensitivity to chemotherapy in others.[37] The effect of HCI-2509 on cell cycle reflects the effect of c-MYC decrease. Cells accumulate in the G0/G1 phase (Figures 5a and b),

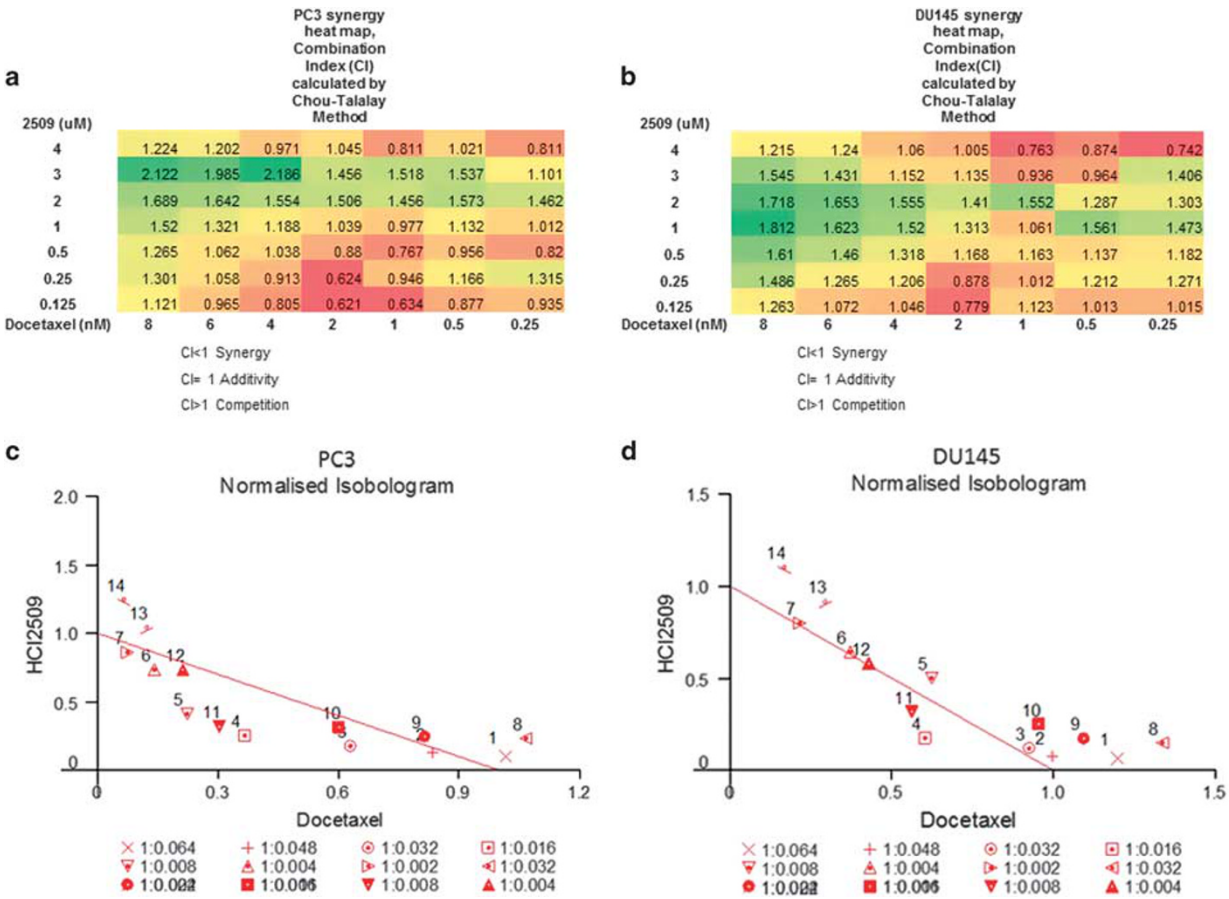

Figure 7. Combination of docetaxel and HCI-2509 in (**a**) PC3 and (**b**) DU145 cells. Combination index (CI) values were calculated by Chou–Talalay equation using CalcuSyn (BIOSOFT, Great Shelford, Cambridge, UK). Heat map was created using the CI values at various combination doses to show points of synergy (CI < 1). Isobologram of CIs in PC3 and DU145 cells in various combinations (**c** and **d**).

correlating with reduction of c-MYC protein. Docetaxel is commonly used in CRPC.[38] It causes a G2/M arrest in the cell cycle owing to the stabilization of microtubules of the mitotic spindle.[39] The presence of one drug may rescue cytotoxicity by the other or may work synergistically by inhibiting different cell populations. We explored the outcome of combining HCI-2509 with docetaxel in CRPC cell lines at various dose levels, and noted differing levels of synergy for the two cell lines at sub-IC_{50} doses and competition at higher concentrations (Figures 7a–d), thus reflecting the complexity of the effect of epigenetic manipulation on cells. Synergy was noted more commonly in PC3 cells than in DU145 cells.

Several different mechanisms have been described to explain chemotherapy resistance in cancer including epithelial–mesenchymal transition with TGF-β-induced LSD1 overexpression.[9] Previous studies have shown activation of c-MYC expression in docetaxel-resistant prostate cancer cell lines.[20] In the castration-resistant setting, use of docetaxel provides an ~3-month average survival advantage[38] with eventual development of toxicity or docetaxel resistance.

As an exploratory objective, we studied the effect of HCI-2509 in the docetaxel-resistant cell line, PC3D12. We first performed cell viability studies confirming docetaxel resistance in PC3D12, as demonstrated by an IC_{50} >50 nM for docetaxel (Figure 8a). There is evidence for the continued efficacy of HCI-2509 in the docetaxel-resistant setting with cytotoxicity (Figure 8b) and potent inhibition of colony formation, as well as a demonstration of increasing H3K9me2 levels and decreasing c-MYC levels with treatment (Figures 8c–e). The efficacy of HCI-2509 in PC3D12 cells suggests that sequencing treatment with LSD1 inhibition after progression on docetaxel in the castration-resistant setting may be a possibility in the future.

In vivo studies demonstrate the antitumor efficacy of HCI-2509 in PC3 xenografts (Figure 6a). HCI-2509 is well tolerated with progressive weight gain in treated mice (Figure 6b), similar to the control arm. There is no significant myelosuppression (Figures 6c–e). Tolerability and myeloid sparing qualities of therapy are an important consideration in the setting of metastatic CRPC and docetaxel-resistant prostate cancer, due to high frequency of bone metastasis leading to marrow replacement, advanced age, comorbidities and myelotoxicity from previous treatments in this patient population. Our *in vivo* study supports use of reversible LSD1 inhibition in this clinical setting.

c-MYC is implicated in stem cell maintenance[40] and, as an oncogenic transcription factor, has been an elusive target for drug development. BET bromodomain inhibition with JQ1 has been shown to downregulate *c-MYC* transcription in prostate cancer and multiple myeloma.[18,41] Here we report LSD1 inhibition as yet another potent epigenetic strategy to inhibit c-MYC expression in the setting of advanced prostate cancer.

We conclude that reversible and potent LSD1 inhibition with HCI-2509 has antitumor efficacy in CRPC cell lines, inhibits c-MYC expression, can sensitize prostate cancer cells to docetaxel and inhibits growth in a docetaxel-resistant prostate cancer cell line. This provides a new therapeutic tool, in the space of an unmet clinical need, in patients who have poorly differentiated prostate

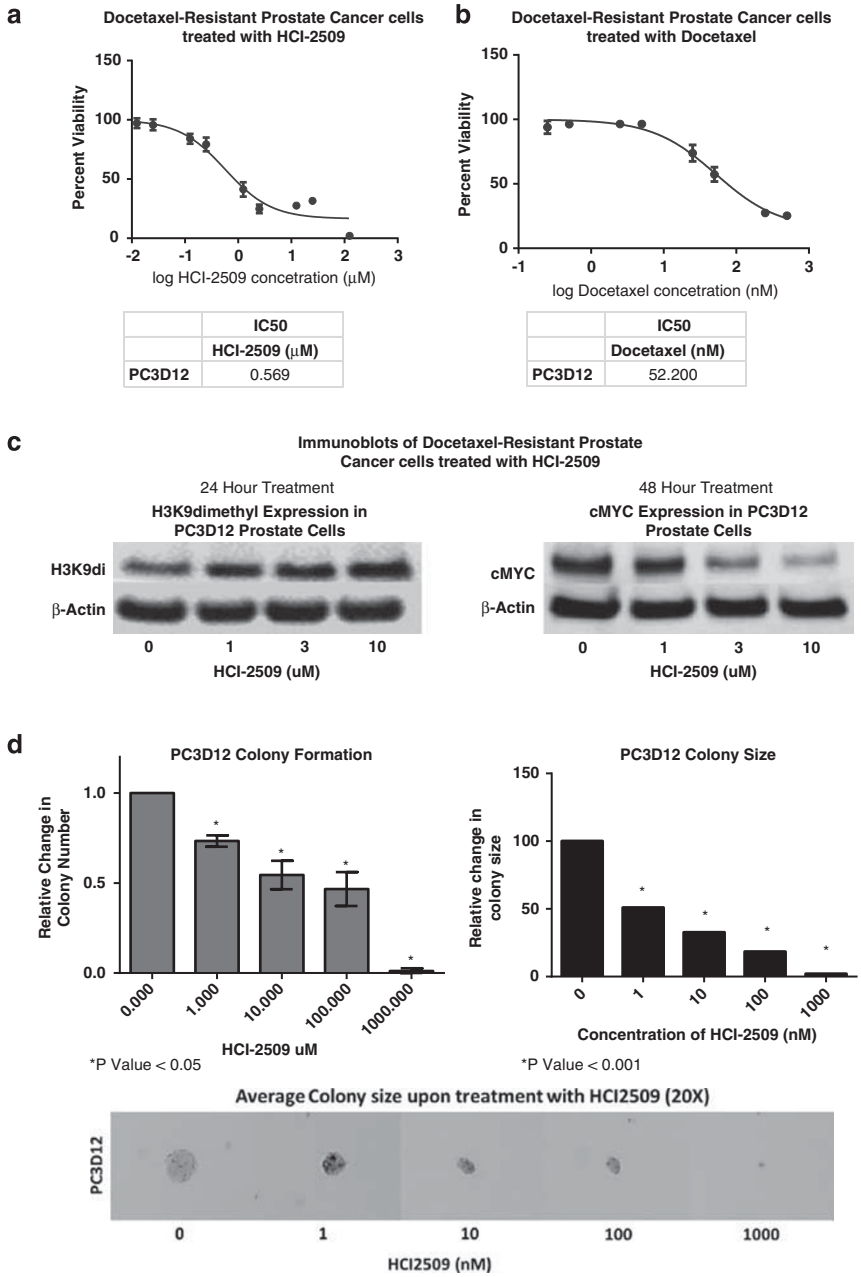

Figure 8. Effect of HCI-2509 on docetaxel-resistant PC3D12 cells. Cell viability studies: dose–response curves showing the percent cell viability at the end of 72 h treatment in PC3D12 treated with (**a**) docetaxel and (**b**) HCI-2509. Colony formation assays show growth inhibition of colonies (**c**) and decreased colony size (**d**) on treatment with HCI-2509. Student's unpaired *t*-tests, using GraphPad Prism software, were used to calculate two-tailed *P*-values for each experiment to determine the statistical significance between untreated and treated samples. The statistically significant *P*-values are labeled in each figure with an asterisk. (**e**) Western blot analysis shows increased H3K9me2 and decreased c-MYC levels on treatment with HCI-2509.

cancer and are facing limited survival with currently available therapies for CRPC. Neuroendocrine differentiation presents yet another challenge in the treatment of prostate cancer.[42] Epigenetic mechanisms such as LSD1-mediated gene regulation may have a role in this phenomenon. This is a possible direction for future studies.

CONFLICT OF INTEREST

SS is a founder and equity holder of Salarius Pharmaceuticals. JB is an equity holder of Salarius Pharmaceuticals. SG's spouse is an equity holder of Salarius Pharmaceuticals. The remaining authors declare no conflicts of interest.

ACKNOWLEDGEMENTS

We thank Dr William Watson and Dr Amanda O'Neill, University College Dublin, Ireland, for providing docetaxel-resistant PC3 cells. This project received financial support from Huntsman Cancer Institute and Huntsman Cancer Foundation. This work was supported by the University of Utah Flow Cytometry Facility in addition to the National Cancer Institute through Award Number 5P30CA042014-24. We are grateful to Ellen Wilson, PhD, for her discussion and critical feedback.

REFERENCES

1 James ND, Spears MR, Clarke NW, Dearnaley DP, De Bono JS, Gale J *et al.* Survival with newly diagnosed metastatic prostate cancer in the 'Docetaxel Era': data from

917 patients in the control arm of the STAMPEDE Trial (MRC PR08, CRUK/06/019). *Eur Urol* 2015; **67**: 1028–1038.
2 Flaig TW, Potluri RC, Ng Y, Todd MB, Mehra M. Treatment evolution for metastatic castration-resistant prostate cancer with recent introduction of novel agents: retrospective analysis of real-world data. *Cancer Med* 2015; **5**: 182–191.
3 Siegel RL, Miller KD, Jemal A. Cancer statistics, 2016. *CA Cancer J Clin* 2016; **66**: 7–30.
4 Lee MG, Wynder C, Cooch N, Shiekhattar R. An essential role for CoREST in nucleosomal histone 3 lysine 4 demethylation. *Nature* 2005; **437**: 432–435.
5 Wang Y, Zhang H, Chen Y, Sun Y, Yang F, Yu W *et al.* LSD1 is a subunit of the NuRD complex and targets the metastasis programs in breast cancer. *Cell* 2009; **138**: 660–672.
6 Metzger E, Wissmann M, Yin N, Muller JM, Schneider R, Peters AH *et al.* LSD1 demethylates repressive histone marks to promote androgen-receptor-dependent transcription. *Nature* 2005; **437**: 436–439.
7 Wang Q, Li W, Zhang Y, Yuan X, Xu K, Yu J *et al.* Androgen receptor regulates a distinct transcription program in androgen-independent prostate cancer. *Cell* 2009; **138**: 245–256.
8 Wu X, Deng F, Li Y, Daniels G, Du X, Ren Q *et al.* ACSL4 promotes prostate cancer growth, invasion and hormonal resistance. *OncoTarget* 2015; **6**: 44849–44863.
9 McDonald OG, Wu H, Timp W, Doi A, Feinberg AP. Genome-scale epigenetic reprogramming during epithelial-to-mesenchymal transition. *Nat Struct Mol Biol* 2011; **18**: 867–874.
10 Kahl P, Gullotti L, Heukamp LC, Wolf S, Friedrichs N, Vorreuther R *et al.* Androgen receptor coactivators lysine-specific histone demethylase 1 and four and a half LIM domain protein 2 predict risk of prostate cancer recurrence. *Cancer Res* 2006; **66**: 11341–11347.
11 Domingo-Domenech J, Vidal SJ, Rodriguez-Bravo V, Castillo-Martin M, Quinn SA, Rodriguez-Barrueco R *et al.* Suppression of acquired docetaxel resistance in prostate cancer through depletion of notch- and hedgehog-dependent tumor-initiating cells. *Cancer Cell* 2012; **22**: 373–388.
12 Koivisto P, Kononen J, Palmberg C, Tammela T, Hyytinen E, Isola J *et al.* Androgen receptor gene amplification: a possible molecular mechanism for androgen deprivation therapy failure in prostate cancer. *Cancer Res* 1997; **57**: 314–319.
13 Edwards J, Krishna NS, Grigor KM, Bartlett JM. Androgen receptor gene amplification and protein expression in hormone refractory prostate cancer. *Br J Cancer* 2003; **89**: 552–556.
14 Antonarakis ES, Lu C, Wang H, Luber B, Nakazawa M, Roeser JC *et al.* AR-V7 and resistance to enzalutamide and abiraterone in prostate cancer. *N Engl J Med* 2014; **371**: 1028–1038.
15 Dehm SM, Schmidt LJ, Heemers HV, Vessella RL, Tindall DJ. Splicing of a novel androgen receptor exon generates a constitutively active androgen receptor that mediates prostate cancer therapy resistance. *Cancer Res* 2008; **68**: 5469–5477.
16 Abreu-Martin MT, Chari A, Palladino AA, Craft NA, Sawyers CL. Mitogen-activated protein kinase kinase kinase 1 activates androgen receptor-dependent transcription and apoptosis in prostate cancer. *Mol Cell Biol* 1999; **19**: 5143–5154.
17 Craft N, Shostak Y, Carey M, Sawyers CL. A mechanism for hormone-independent prostate cancer through modulation of androgen receptor signaling by the HER-2/neu tyrosine kinase. *Nat Med* 1999; **5**: 280–285.
18 Gao L, Schwartzman J, Gibbs A, Lisac R, Kleinschmidt R, Wilmot B *et al.* Androgen receptor promotes ligand-independent prostate cancer progression through c-Myc upregulation. *PLoS One* 2013; **8**: e63563.
19 Bernard D, Pourtier-Manzanedo A, Gil J, Beach DH. Myc confers androgen-independent prostate cancer cell growth. *J Clin Invest* 2003; **112**: 1724–1731.
20 Hatano K, Yamaguchi S, Nimura K, Murakami K, Nagahara A, Fujita K *et al.* Residual prostate cancer cells after docetaxel therapy increase the tumorigenic potential via constitutive signaling of CXCR4, ERK1/2 and c-Myc. *Mol Cancer Res* 2013; **11**: 1088–1100.
21 Festuccia C, Gravina GL, D'Alessandro AM, Muzi P, Millimaggi D, Dolo V *et al.* Azacitidine improves antitumor effects of docetaxel and cisplatin in aggressive prostate cancer models. *Endocr-Relat Cancer* 2009; **16**: 401–413.
22 Hwang JJ, Kim YS, Kim MJ, Kim DE, Jeong IG, Kim C-S. Histone deacetylase inhibitor potentiates anticancer effect of docetaxel via modulation of Bcl-2 family proteins and tubulin in hormone refractory prostate cancer cells. *J Urol* 2010; **184**: 2557–2564.
23 Alimirah F, Chen J, Basrawala Z, Xin H, Choubey D. DU-145 and PC-3 human prostate cancer cell lines express androgen receptor: implications for the androgen receptor functions and regulation. *FEBS Lett* 2006; **580**: 2294–2300.
24 Hu Y, Gu Y, Wang H, Huang Y, Zou YM. Integrated network model provides new insights into castration-resistant prostate cancer. *Scientific Rep* 2015; **5**: 17280.
25 Sankar S, Theisen ER, Bearss J, Mulvihill T, Hoffman LM, Sorna V *et al.* Reversible LSD1 inhibition interferes with global EWS/ETS transcriptional activity and impedes Ewing sarcoma tumor growth. *Clin Cancer Res* 2014; **20**: 4584–4597.
26 Fiskus W, Sharma S, Shah B, Portier BP, Devaraj SGT, Liu K *et al.* Highly effective combination of LSD1 (KDM1A) antagonist and pan-histone deacetylase inhibitor against human AML cells. *Leukemia* 2014; **28**: 2155–2164.
27 Theisen ER, Gajiwala S, Bearss J, Sorna V, Sharma S, Janat-Amsbury M. Reversible inhibition of lysine specific demethylase 1 is a novel anti-tumor strategy for poorly differentiated endometrial carcinoma. *BMC Cancer* 2014; **14**: 752.
28 Sorna V, Theisen ER, Stephens B, Warner SL, Bearss DJ, Vankayalapati H *et al.* High-throughput virtual screening identifies novel *N*'-(1-phenylethylidene)-benzohydrazides as potent, specific, and reversible LSD1 inhibitors. *J Med Chem* 2013; **56**: 9496–9508.
29 O'Neill AJ, Prencipe M, Dowling C, Fan Y, Mulrane L, Gallagher WM *et al.* Characterisation and manipulation of docetaxel resistant prostate cancer cell lines. *Mol Cancer* 2011; **10**: 126.
30 Zheng YC, Ma J, Wang Z, Li J, Jiang B, Zhou W *et al.* A systematic review of histone lysine-specific demethylase 1 and its inhibitors. *Med Res Rev* 2015; **35**: 1032–1071.
31 Wang M, Liu X, Guo J, Weng X, Jiang G, Wang Z *et al.* Inhibition of LSD1 by pargyline inhibited process of EMT and delayed progression of prostate cancer in vivo. *Biochem Biophys Res Commun* 2015; **467**: 310–315.
32 Wu CY, Hsieh CY, Huang KE, Chang C, Kang HY. Cryptotanshinone down-regulates androgen receptor signaling by modulating lysine-specific demethylase 1 function. *Int J Cancer* 2012; **131**: 1423–1434.
33 Willmann D, Lim S, Wetzel S, Metzger E, Jandausch A, Wilk W *et al.* Impairment of prostate cancer cell growth by a selective and reversible lysine-specific demethylase 1 inhibitor. *Int J Cancer* 2012; **131**: 2704–2709.
34 Wang J, Lu F, Ren Q, Sun H, Xu Z, Lan R *et al.* Novel histone demethylase LSD1 inhibitors selectively target cancer cells with pluripotent stem cell properties. *Cancer Res* 2011; **71**: 7238–7249.
35 Adamo A, Sese B, Boue S, Castano J, Paramonov I, Barrero MJ *et al.* LSD1 regulates the balance between self-renewal and differentiation in human embryonic stem cells. *Nat Cell Biol* 2011; **13**: 652–659.
36 von Bueren AO, Oehler C, Shalaby T, von Hoff K, Pruschy M, Seifert B *et al.* c-MYC expression sensitizes medulloblastoma cells to radio- and chemotherapy and has no impact on response in medulloblastoma patients. *BMC Cancer* 2011; **11**: 74.
37 Leonetti C, Biroccio A, Candiloro A, Citro G, Fornari C, Mottolese M *et al.* Increase of cisplatin sensitivity by c-myc antisense oligodeoxynucleotides in a human metastatic melanoma inherently resistant to cisplatin. *Clin Cancer Res* 1999; **5**: 2588–2595.
38 Berthold DR, Pond GR, Soban F, de Wit R, Eisenberger M, Tannock IF. Docetaxel plus prednisone or mitoxantrone plus prednisone for advanced prostate cancer: updated survival in the TAX 327 study. *J Clin Oncol* 2008; **26**: 242–245.
39 Herbst RS, Khuri FR. Mode of action of docetaxel—a basis for combination with novel anticancer agents. *Cancer Treat Rev* 2003; **29**: 407–415.
40 Araki R, Hoki Y, Uda M, Nakamura M, Jincho Y, Tamura C *et al.* Crucial role of c-Myc in the generation of induced pluripotent stem cells. *Stem Cells* 2011; **29**: 1362–1370.
41 Delmore Jake E, Issa Ghayas C, Lemieux Madeleine E, Rahl Peter B, Shi J, Jacobs Hannah M *et al.* BET bromodomain inhibition as a therapeutic strategy to target c-Myc. *Cell* 2011; **146**: 904–917.
42 Sun Y, Niu J, Huang J. Neuroendocrine differentiation in prostate cancer. *Am J Transl Res* 2009; **1**: 148–162.